Regular Article

Lanthania Colloidal Nanoparticles: Hydrothermal Synthesis, Structural, and Rheological Properties

E.K. Goharshadi[a,b,*], T. Mahvelati[a] and M. Yazdanbakhsh[b]

[a]Dept. of Chemistry, Ferdowsi University of Mashhad, Mashhad 91779, Iran
[b]Center of Nano Research, Ferdowsi University of Mashhad, Iran
(Received 11 July 2015, Accepted 14 January 2016)

In this work, for the first time, the rheological properties of nanofluids of lanthania nanoparticles (NPs) in ethylene glycol (EG) as functions of shear rate, volume fraction, and temperature were measured. The results showed that both EG and the nanofluids behave as non-Newtonian fluids at lower shear rates and transform to Newtonian fluids at higher shear rates. The values of viscosity for both EG and the nanofluids decrease with raising temperature. The viscosity of nanofluids increases with increasing the volume fraction of lanthania NPs. A maximum of 66.4% increase in viscosity of EG at 25 °C and shear rate of 60 s^{-1} was observed when 5% v/v of lanthania NPs was added. The nearly pure hexagonal lanthania NPs were successfully synthesized using hydrothermal method. The NPs were characterized using seven techniques including X-ray powder diffraction, transmission electron microscopy, field emission scanning electron microscopy, energy dispersive X-ray spectroscopy, Fourier transform infrared spectroscopy, far infrared spectroscopy, and ultraviolet-visible absorption spectroscopy.

INTRODUCTION

Nanofluids, suspensions of nanometerials in base fluids such as water and ethylene glycol (EG) have novel properties. They are potentially useful for various applications including engineering, biology, and medicine [1-11]. Having knowledge of the transport properties of nanofluids such as thermal conductivity and rheological properties are very important for their applications. Several research groups studied various characteristics of fluid flow and heat transfer behavior of nanofluids [12-16].

The viscosity of nanofluids is very important for their industrial applications. For example, knowledge of viscosity is essential for establishing an adequate pumping power as well as the convective heat transfer coefficient. The viscosity of nanofluids depends on several factors including temperature, shear rate, γ^o, and particle size, shape, and

_____
*Corresponding author. E-mail: gohari@um.ac.ir

concentration of the nanoparticles (NPs). Nanofluids can be divided to Newtonian and non-Newtonian fluids according to their behavior with respect to the variation in shear rate. Newtonian fluids have the following features:
1. Their viscosity, η, is dependent only on temperature but not on shear rate.
2. The ratio of the shear stress, τ, to shear rate is a constant which is called viscosity. In other words, they obey Newton's law of viscosity:

$$\tau = \eta \gamma^{0} \tag{1}$$

On the other hand, the viscosity of a non-Newtonian fluid depends on the shear rate as well as temperature. The aims of the present work are preparing La$_2$O$_3$ NPs using hydrothermal method and measuring the rheological properties of La$_2$O$_3$-EG nanofluis as functions of temperature, volume fraction, and shear rate. Lanthanum(III) oxide (lanthania), La$_2$O$_3$ has multiple

polymorphs including hexagonal and cubic forms. Lanthanum oxide is used to develop ferroelectric materials such as La-doped $Bi_4Ti_3O_{12}$. Often, the optical glasses are doped with La_2O_3 to improve the glass' refractive index, chemical durability, and mechanical strength. It is an ingredient for the manufacture of piezoelecteric and thermoelectric materials [17]. Automobile exhaust-gas converters contain La_2O_3 [18].

EXPERIMENTAL

Materials

LaCl$_3$, 7H$_2$O (BDH) was used as the starting material. Ammonia solution (Merck, 25% NH$_3$) was utilized as a hydrolysis agent. EG (Merck) was used as a base fluid. Hexadecyltrimethyl ammonium bromide (CTAB) (Merck) was used as a surfactant. All chemicals were of analytical grade and used as received without further purification.

Synthesis Procedure

For preparation of La_2O_3NPs, 0.2730 g of CTAB was first put into 30 ml deionized water under magnetic stirring at room temperature. Then, 1.58 mmol LaCl$_3$.7H$_2$O was added while stirring to form a homogeneous transparent solution and 25% ammonia was added dropwise to the above solution to adjust the pH of the solution at 8.5. After vigorous stirring for 2 h, the system was transferred into a Teflon-lined stainless steel autoclave, sealed, and maintained at 80 ℃ for 24 h. The resultant white solid product was centrifuged, washed with deionized water, and dried in vacuum oven at 80 ℃ for 4 h. Finally, the obtained powder was calcined at 800 ℃ for 4 h.

In order to prepare lanthania-EG nanofluid, a certain amount of La_2O_3 and CTAB were added to 50 ml of EG and irradiated by ultrasonic waves with intensity of 100 for 15 min at 25 ℃.

Characterization Techniques

The powder phase of the NPs was determined by means of a Bruker/D8 Advanced diffractometer in the 2θ range from 20° to 80°, by step of 0.04 degree, with graphite monochromatic Cu Kα radiation (λ = 1.541 Å).

The transmission electron microscopy (TEM) analysis of the sample was taken using a LEO 912 AB instrument.

The electron beam accelerating voltage was 120 kV. The field emission scanning electron microscopy (FE-SEM) analysis of the sample was performed by Hitachi S-4160 instrument. The energy-dispersive X-ray (EDX) analysis of the sample was obtained using an Inca 400 instrument.

The Fourier transform infrared (FT-IR) spectrum of the fabricated lanthania NPs was recorded at room temperature with a KBr pellet on a Shimadzu 4300 spectrometer ranging from 450-4000 cm^{-1}. The Far-IR spectrum of the NPs in the region 600-250 cm^{-1} was obtained using a Thermo Nicolet EXUS 870 FT-IR spectrometer equipped with DTGS/polyethylene detector and a solid substrate beam splitter. The spectrum was collected with a resolution of 4 cm^{-1}.

The ultraviolet-visible (UV-Vis) absorption spectrum of the sample was obtained using an Agilent photodiode-array model 8453 equipped with a glass of 1 cm path length. The spectrum was recorded at room temperature in air within the range 200-600 nm.

The viscosity of the nanofluids of lanthania NPs in EG was measured using a Brookfield Viscometer (LV DV-II+Pro EXTRA). Accurate temperature control is a fundamental requirement for the rheological measurements. In the current research, the water jacket was connected to a circulating cooling water bath (BL 7100, Major Science) to control the water temperature.

RESULTS AND DISCUSSION

Characterization

Figure 1a shows the XRD pattern of the prepared NPS. All the diffraction peaks were indexed to the hexagonal phase with the lattice parameters of $a = b = 0.3973$ nm and $c = 0.6129$ nm (JCPDS-050602). The strong and sharp diffraction peaks indicate the good crystallinity of the NPs. The average crystallite size, D, can be calculated by the well-known Scherrer's formula:

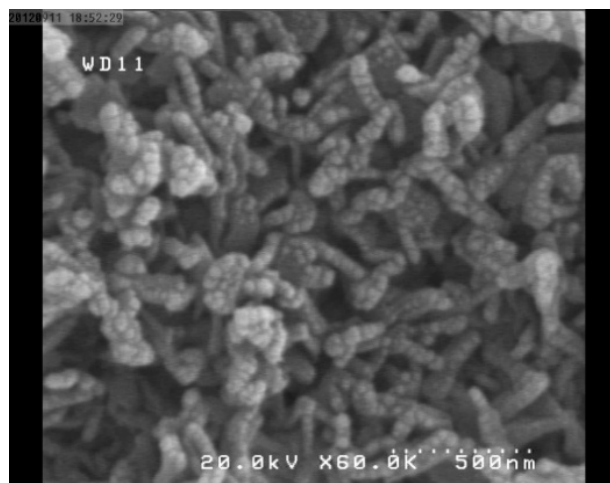$$D_{hkl} = \frac{k \times \lambda}{\beta_{hkl} \times \cos\theta_{hkl}} \tag{2}$$

where D_{hkl} is the crystlallite size perpendicular to the normal line of (hkl) plane, k is a constant and equals 0.9. β_{hkl} is the full width at half maximum (FWHM) of the (hkl) diffraction
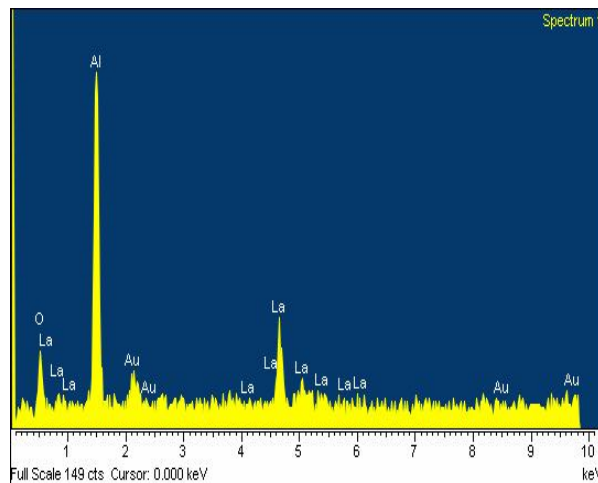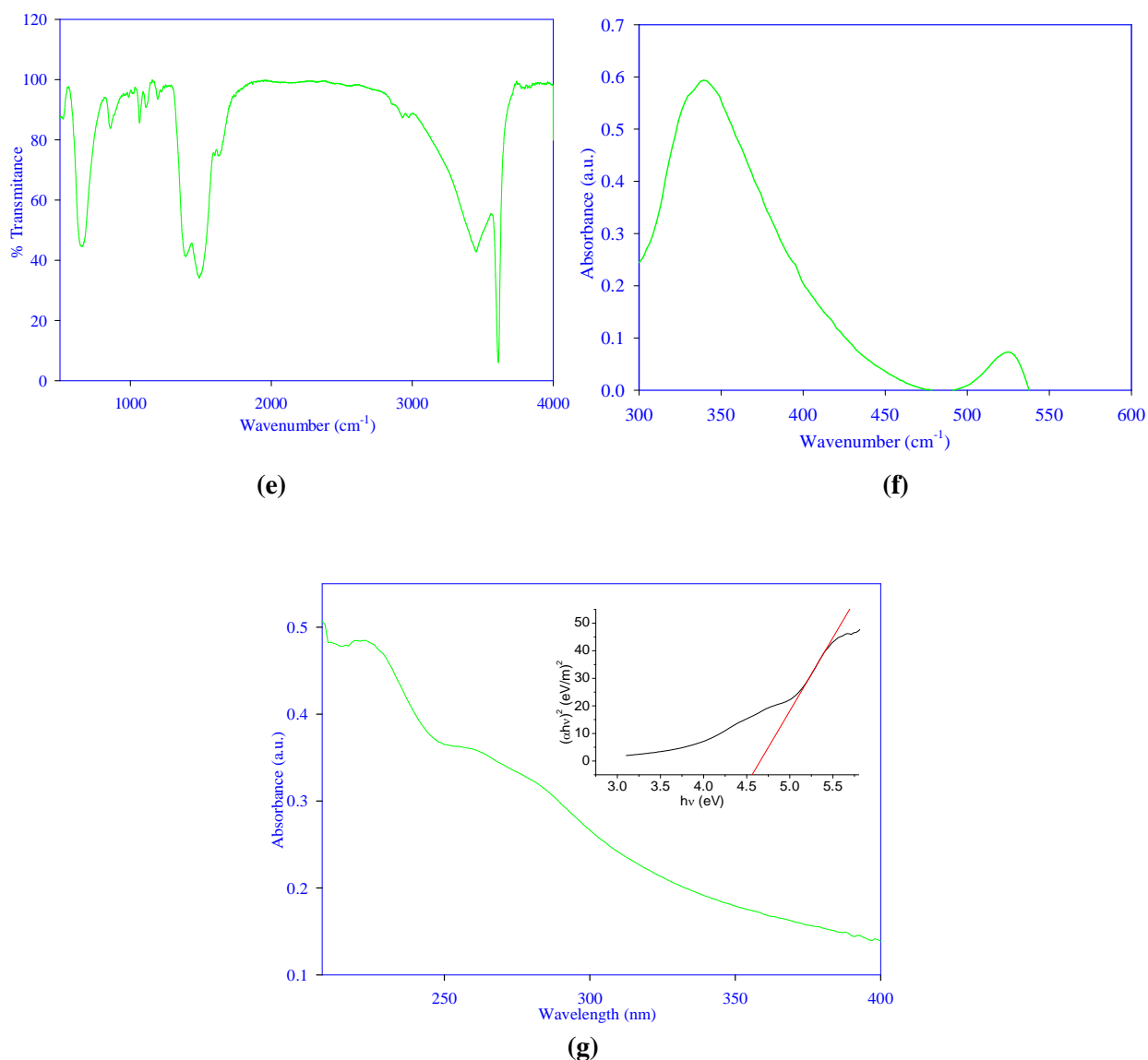
(a)

(b)

(c)

**(d)**

(e)

(f)

(g)
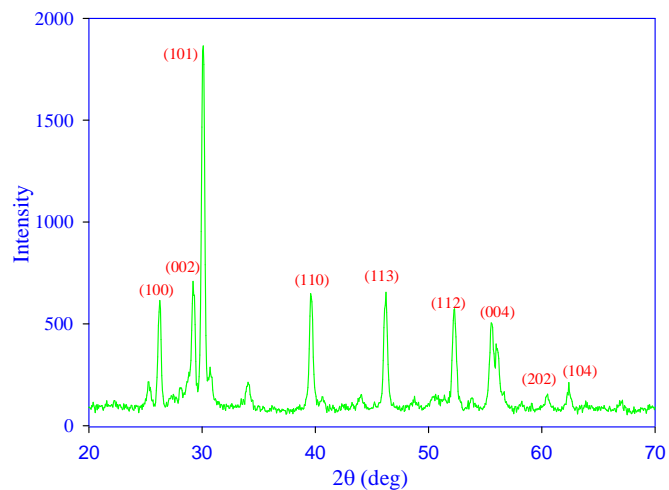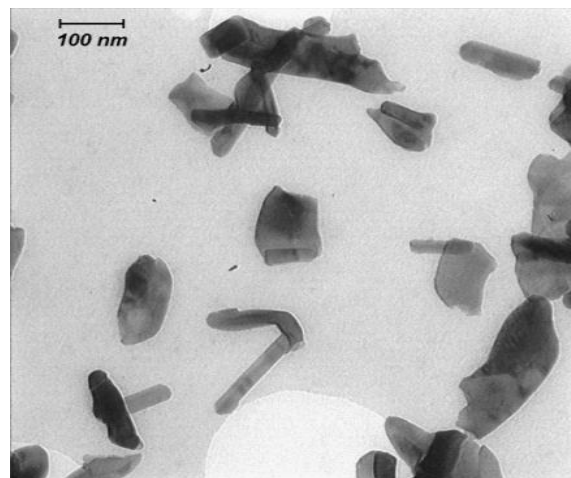
Fig. 1. (a) XRD pattern (b) TEM image (c) FE-SEM image (d) EDX spectrum (e) FTIR spectrum (f) Far-IR spectrum (g) UV-Vis absorption spectrum of lanthania NPs in ethanol (Plot of $(\alpha h\upsilon)^2$ *vs*. photon energy is shown in the inset).

peak, θ_{hkl} is the Bragg angle of (*hkl*) peak, and λ is the wavelength of X-ray. The crystallite size of the lanthania NPs was 29 nm.

As TEM and FE-SEM images, Figs. 1b, and 1c, respectively show the NPs have rod like structure. The EDX of the sample was given in Fig. 1d. The EDX spectrum shows the presence of lanthanum, oxygen, aluminum, and gold. The Al peak was originated from the

aluminum covering slab which was applied during the sample preparation to avoid pollution and impurities. The Au peak was resulted from gold coating the sample. The EDX analysis indicates that there is no impurity in the sample. Figure 1e shows the FT-IR spectrum of the lanthania NPs. The bands around 3421 cm^{-1} can be attributed to the O-H vibration of water. The sharp peak around 1600 cm^{-1} is due to the bending mode of H-O-H.
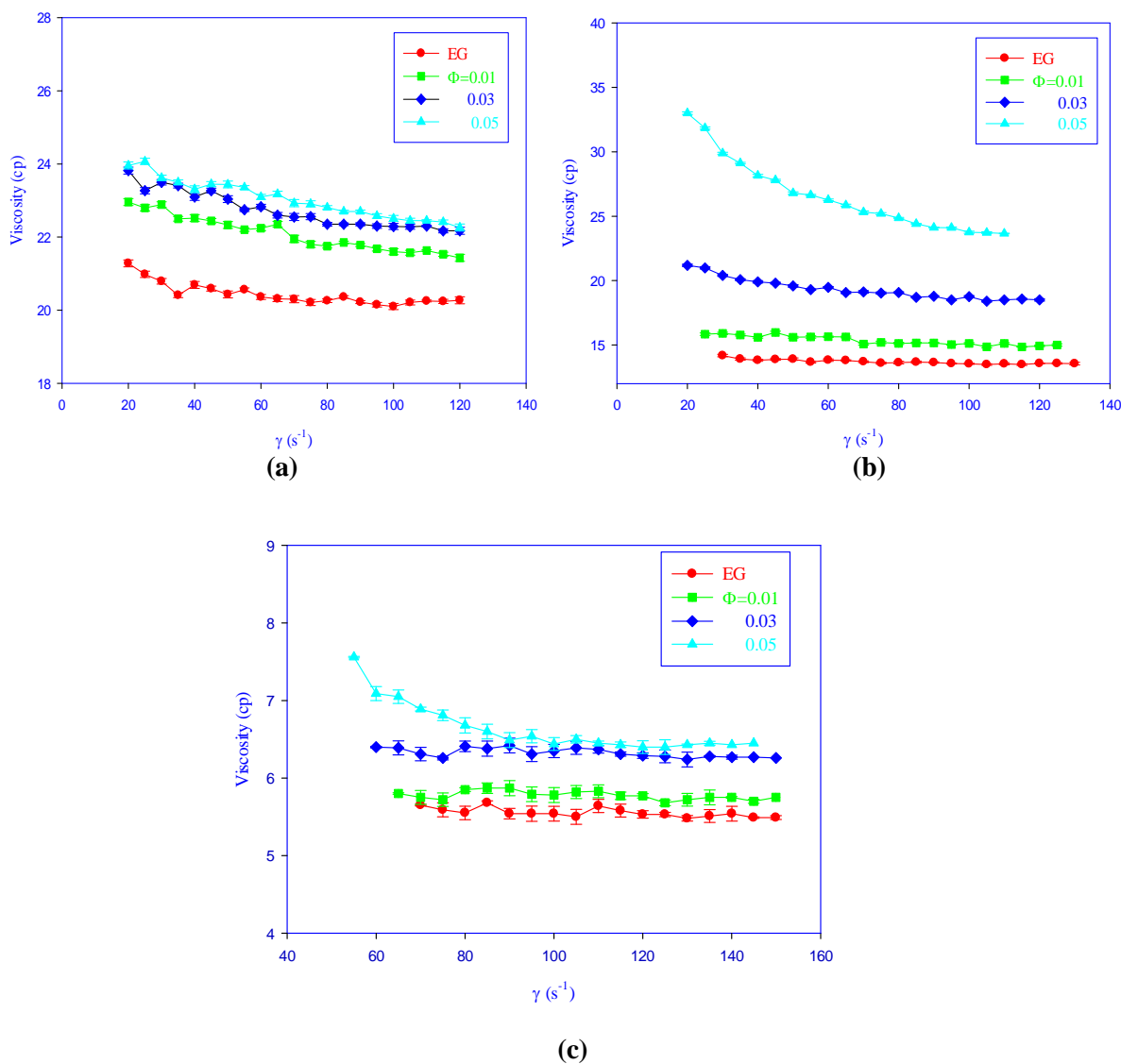
Fig. 2. Viscosity of EG and in EG *vs.* shear rate at different volume fractions at (a) 10 (b) 25 (c) 50 °C.

The band at around 646 cm^{-1} is assigned to the La-O vibration [19]. Figure 1f displays the Far-IR spectrum of the lanthania NPs. The broad peak in the range 550-500 cm^{-1} is assigned to the La-O stretching vibration.

Figure 1g shows the UV-Vis absorption spectrum of the sample. The maximum absorption wavelength for lanthania NPs is 204 nm. The optical band gap, E_g, can be estimated using Tauc's equation [20]:

$$(\alpha h\upsilon)^n = B(h\upsilon - E_g) \tag{3}$$

where $h\upsilon$ and α stand for the photon energy and the absorption coefficient, respectively. B is a constant. The parameter n represents the nature of optical transition, $n = 2$ for direct transitions and $n = 1/2$ for indirect transitions. Plotting $(\alpha h\upsilon)^n$ against the photon energy and extrapolating the linear region of the curve to the x-axis gives the optical band gap. Lanthania is a direct semiconductor. The variation of $(\alpha h\upsilon)^2$ with photon energy for aqueous lanthania dispersion is shown as the inset of Fig. 1g. The estimated band gap of lanthania NPs was calculated to be

4.69 eV whereas the value for the bulk of lanthania is 4.3 eV. Hence, the band gap increases with decreasing size due to the quantum confinement effect of lanthania NPs [21].

Rheological Studies

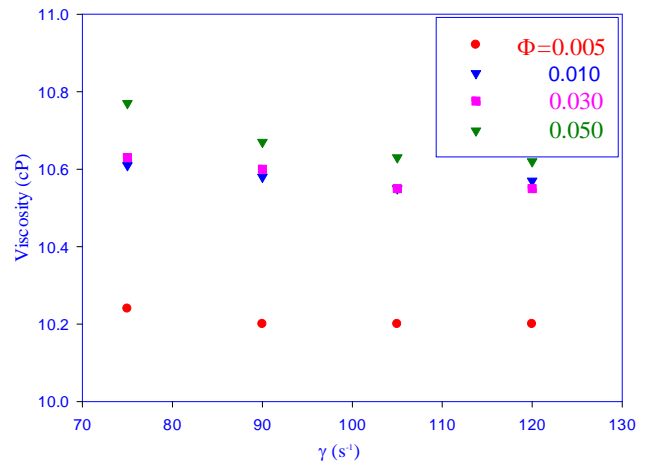The viscosity of both EG and nanofluids of lanthania NPs in EG was measured at different volume fractions, ϕ, and temperatures. Figures 2a, 2b and 2c show the measured viscosity as a function of shear rate for EG and lanthania-EG nanofluids at 10, 25 and 50 °C. As the figures shows, both EG and the nanofluids act as non-Newtonian fluids at low shear rates but as shear rate increases more than 65 s^{-1}, they represent the Newtonian behavior. As shear rate increases, the individual particles of aggregate start to break apart and align in the direction of the shearing flow and hence the viscosity decreases. Also, the values of viscosity for both EG and nanofluids decrease with increasing temperature. The results also show that viscosity increases with increasing volume fraction. A maximum of 66.4% increase in viscosity of EG at 25 °C and shear rate of 60 s^{-1} was observed when the volume fraction of NPs was 5%.

Figure 3 shows the viscosity of nanofluids as a function of volume fraction at different shear rates and at 30 °C. The viscosity of nanofluids increases with increasing volume fraction. By increasing the concentration of lanthania NPs in EG, the system becomes progressively chaotic as more aggregates form and hence viscosity increases.

Figure 4 illustrates the measured values of viscosity in comparison with the predicted values from the theoretical models of Einstein [22], Brinkman [23], and Batchelor [24]. It is plausible to say that the models overestimate the viscosity of nanofluids. The reason is that the calculated values of viscosity according to the models depend only on the viscosity of the base fluid and the volume fraction of the nanoparticles whereas the results of many experimental studies showed that the viscosity of nanofluids also depends on the size, shape , morphology, and kind of NPs and temperature [11].

The temperature dependence of viscosity of nanofluids is described by Vogel-Tammann-Fulcher (VTF) equation [20]:

$$\ln \eta = A + \frac{1000B}{(T + C)} \tag{4}$$

Fig. 3. Viscosity of nanofluids of lanthania NPs as a function of volume fraction at different shear rates at 30 °C.
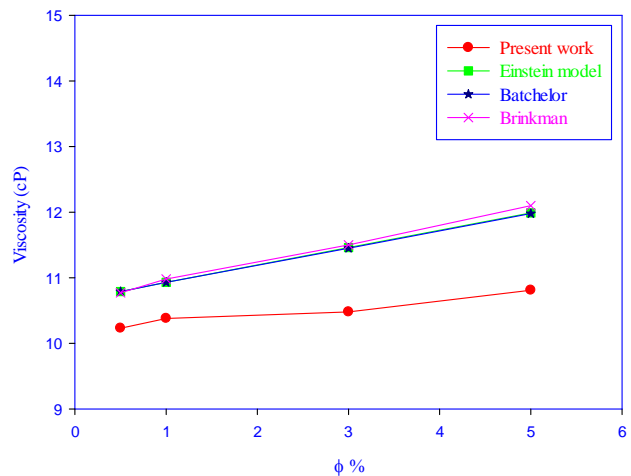

Fig. 4. Comparison between the experimental data for viscosity of nanofluids of lanthania NPs at 20 °C and shear rate of 80 s^{-1} and the viscosity models.

where *A*, *B* and *C* are constants. *A* is the value of *lnη* at the infinite temperature. The experimental data at a constant shear rate were fitted well with VTF equation (Fig. 5). The fitting parameters are summarized in Table 1.
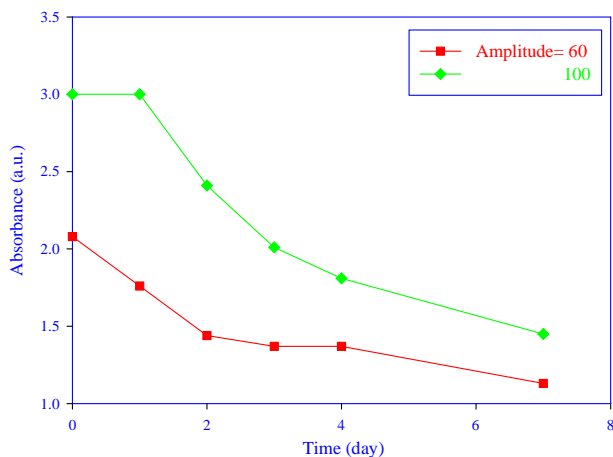
Stability of Nanofluids

The stability of nanofluids was examined by UV-Vis

148
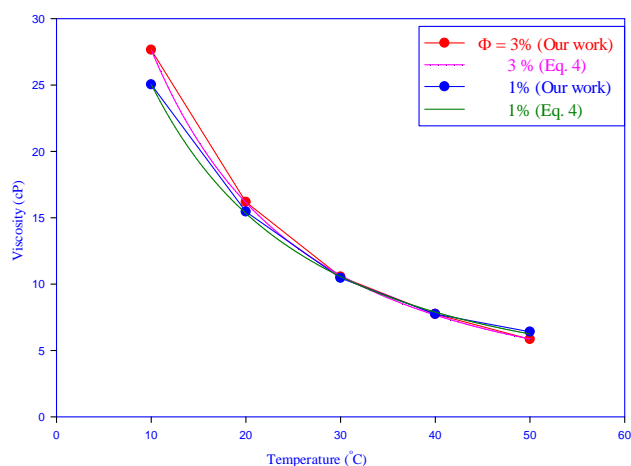
Fig. 5. Viscosity of nanofluids of lanthania NPs as a function of temperature at a constant shear rate of 80 s^{-1}. The symbols and lines are the experimental and calculated values using VTF equation, respectively.
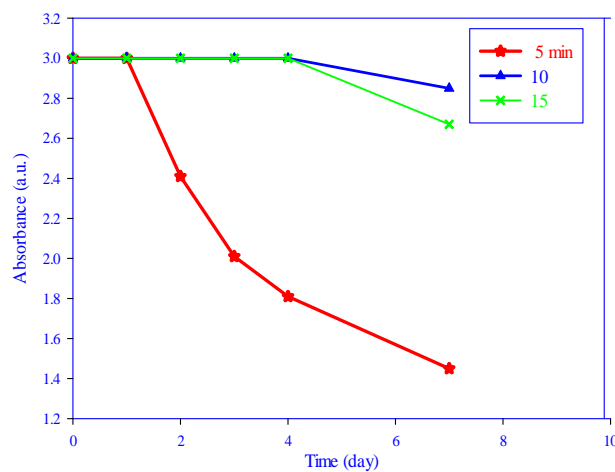
Fig. 7. The absorbance of nanofluids of lanthania NPs ($\Phi = 0.01$) *vs.* wavelength at 25 °C with ultrasound intensity of 100 for different ultrasound irritation times.

intensity of ultrasound is important for production of nanofluids, however the time of the irradiation is more important.

Figure 7 shows that by increasing the time of irradiation at intensity 100, the stability of nanofluid increases. Of course, there is no noticeable difference between 10 and 15 min irradiation. Therefore, the irradiation intensity and time were chosen 100 and 15 min, respectively to prepare nanofluids in this study.

CONCLUSIONS

The following important conclusions can be drawn from the present study:

1. The nearly pure hexagonal lanthania nanorods were successfully synthesized using hydrothermal method. The samples were characterized using several techniques.

2. The rheological properties of lanthania-EG nanofluids as functions of shear rate, volume fraction, and temperature were measured. The results showed that both EG and the nanofluids behave as non-Newtonian fluids at lower shear rates and transform to Newtonian fluids at higher shear rates. A maximum of 66.4% increase in viscosity of EG at 25 °C and shear rate of 60 s^{-1} was observed when volume

Fig. 6. The absorbance of nanofluids of lanthania NPs ($\Phi = 0.01$) *vs.* wavelength at 25 °C for ultrasound intensities of 60 and 100 after 5 min.

spectroscopy. For this purpose, the effect of time and intensity of ultrasound irradiation on nanofluid stability were investigated within one week. Figure 6 shows that by increasing the ultrasound intensity from 60-100, the stability of nanofluid increases slightly. This indicates that the

Table 1. The Empirical Constants of VTF Equation

Nanofluid	A	B	C	R^2
La_2O_3 + EG ($\Phi = 0.03$, $\gamma^o = 80$ s^{-1})	-0.8402	0.2798	-215.8793	0.9999
La_2O_3 + EG ($\Phi = 0.01$, $\gamma^o = 80$ s^{-1})	-0.3395	0.2225	-220.6794	0.9993

fraction of the NPs was 5%. This is an advantage for EG-based materials like aerosol paint concentrates, agricultural chemicals, antifreeze preparations, automobile body polish and cleaners, disinfectants, glass window cleaning preparations, lubricating oils; *i.e.* the decrease in the viscosity of EG with increasing temperature is compensated by loading the NPs [2].

3. The values of viscosity of both EG and the nanofluids decrease with raising temperature. The viscosity of nanofluids increases with increasing the volume fraction of the NPs.

ACKNOWLEDGEMENTS

REFERENCES

[1] Goharshadi, E. K.; Azizi-Toupkanloo, H., Silver colloid nanoparticles: Ultrasound-assisted synthesis, electrical and rheological properties, *Powder Technol.* **2013**, *237*, 97-101, DOI: 10.1016/j.powtec.2012.12.059.

[2] Azizi-Toupkanloo, H.; Goharshadi, E. K.; Nancarrow, P., Structural, electrical and rheological properties of palladium/silver bimetallic nanoparticles prepared by conventional and ultrasonic-assisted reduction methods, *Adv. Powder Technol.* **2014**, *25*, 801-810, DOI: 10.1016/j.apt.2013.11.015.

[3] Abareshi, M.; Goharshadi, E. K.; Zebarjad, S. M.; Fadafan, H. K.; Youssefi, A., Fabrication,

characterization and measurement of thermal conductivity of Fe_3O_4 nanofluids, *J. Magn. Magn. Mater.* **2010**, *322*, 3895-3901, DOI: 10.1016/j.jmmm.2010.08.016.

[4] Jalal, R.; Goharshadi, E. K.; Abareshi, M.; Moosavi, M.; Yousefi, A.; Nancarrow, P., ZnO nanofluids: Green synthesis, characterization, and antibacterial activity, *Mater. Chem. Phys.* **2010**, *121*, 198-201, DOI: 10.1016/j.matchemphys.2010.01.020.

[5] Moosavi, M.; Goharshadi, E. K.; Youssefi, A., Fabrication, characterization, and measurement of some physicochemical properties of ZnO nanofluids, *Int. J. Heat Fluid Flow* **2010**, *31*, 599-605, DOI: 10.1016/j.ijheatfluidflow.2010.01.011.

[6] Goharshadi, E. K.; Hadadian, M., Effect of calcination temperature on structural, vibrational, optical, and rheological properties of zirconia nanoparticles, *Ceram. Int.* **2012**, *38*, 1771-1777, http://dx.doi.org/10.1016/j.ceramint.2011.09.063.

[7] Yeganeh, M.; Shahtahmasebi, N.; Kompany, A.; Goharshadi, E.; Youssefi, A.; Šiller, L., olume fraction and temperature variations of the effective thermal conductivity of nanodiamond fluids in deionized water, *Int. J. Heat Mass Transfer* **2010**, *53*, 3186-3192, DOI: 10.1016/j.ijheatmasstransfer.2010.03.008.

[8] Moghaddam, M. B.; Goharshadi, E. K.; Entezari, M. H.; Nancarrow, P., Preparation, characterization, and rheological properties of graphene-glycerol nanofluids, *Chem. Eng. J.* **2013**, *231*, 365-372, DOI: 10.1016/j.cej.2013.07.006.

[9] Hadadian, M.; Goharshadi, E. K.; Youssefi, A., Electrical conductivity, thermal conductivity, and rheological properties of graphene oxide-based

nanofluids, *J. Nanopart. Res.* **2014**, *16*, 1-17, DOI: 10.1007/S11051-014-2788-1.

[10] Mahdizadeh, S. J.; Goharshadi, E. K., Thermal conductivity and heat transport properties of graphene nanoribbons, *J. Nanopart. Res.* **2014**, *16*, 1-12, DOI: 10.1007/S11051-014-2553-5.

[11] Goharshadi, E. K.; Ahmadzadeh, H.; Hadadian, M.; Samiee, S., Nanofluids for Heat Transfer Enhancement-A Review, *Phys. Chem. Res.* **2013**, *1*, 1-33, DOI: 10.7897/2230-8407.050451.

[12] Mishra, A.; Srivastava, V.; Ram, S., Nonlinear variation of optical absorption and rheological behavior with concentration in dispersed poly(vinyl pyrrolidone) of small molecules in water, *J. Mol. Liq.* **2008**, *137*, 58-63 DOI: 10.1016/j.molliq.2007.03.008.

[13] Yu, W.; France, D. M.; Routbort, J. L.; Choi, S. U., Review and comparison of nanofluid thermal conductivity and heat transfer enhancements, *Heat Transfer Eng.* **2008**, *29*, 432-460, DOI:10.1080/01457630701850851.

[14] Hosseini, M.; Ghader, S., A model for temperature and particle volume fraction effect on nanofluid viscosity, *J. Mol. Liq.* **2010**, *153*, 139-145, DOI: 10.1016/j.molliq.2010.02.003.

[15] Wang, L.; Chen, H.; Witharana, S., Rheology of nanofluids: review, *Recent Pat. Nanotechnol.* **2013**, *7*, 232-246, DOI: 10.2174/1872210507703131127102602.

[16] Mjalli, F. S.; Al-Wahaibi, T.; Al-Hashmi, A. A., Effect of nano-particles on the rheological properties of Reline, *J. Mol. Liq.* **2015**, *206*, 256-261, DOI: 10.1016/j.molliq.2015.02.040.

[17] Cao, J.; Ji, H.; Liu, J.; Zheng, M.; Chang, X.; Ma, X.; Zhang, A.; Xu, Q., Controllable syntheses of hexagonal and lamellar mesostructured lanthanum

oxide, *Mater. Lett.* **2005**, 59, 408-411, DOI: 10.1016/j.molliq.2015.02.040.

[18] Nejad, S. J.; Abolghasemi, H.; Moosavian, M.; Golzary, A.; Maragheh, M., Fractional factorial design for the optimization of hydrothermal synthesis of lanthanum oxide under supercritical water condition, *J. Supercrit. Fluids* **2010**, *52*, 292-297, DOI: 10.1016/j.supflu.2010.01.013.

[19] Zhou, S. -Q.; Ni, R.; Funfschilling, Effects of shear rate and temperature on viscosity of alumina polyalphaolefins nanofluids, D. *J. Appl. Phys.* **2010**, *107*, 054317, DOI: 10.1063/1.3309478.

[20] Timofeeva, E. V.; Routbort, J. L.; Singh, D., Particle shape effects on thermophysical properties of alumina nanofluids, *J. Appl. Phys.* **2009**, 106, 014304, DOI: 10.1063/1.3155999.

[21] Goharshadi, E. K.; Mehrkhah, R.; Nancarrow, P., Synthesis, characterization, and measurement of structural, optical and photoluminescent properties of zinc sulfide, quantum dot, *Mater. Sci. Semicond. Process.* **2013**, *16*, 356-362, DOI: 10.1016/j.mssp.2012.09.012.

[22] Nguyen, C.; Desgranges, F.; Galanis, N.; Roy, G.; Maré, T.; Boucher, S.; Mintsa, H. A., Viscosity data for Al_2O_3-water nanofluid-hysteresis: is heat transfer enhancement using nanofluids reliable? *Int. J. Thermal Sci.* **2008**, *47*, 103-111, DOI: 10.1016/j.ijthermalsci.2007.01.033.

[23] Brinkman, H., The viscosity of concentrated suspensions and solutions, *J. Chem. Phys.* **1952**, *20*, 571-571, DOI: 10.1063/1.1700493.

[24] Batchelor, G., The effect of Brownian motion on the bulk stress in a suspension of spherical particles, *J. Fluid Mech.* **1977**, *83*, 97-117, DOI: 10.1017/S0022112077001062.